

Volumetric Capture

Marcel Bruckner

marcel.bruckner@tum.de

Kevin Bein

kevin.bein@tum.de

Moiz Sajid

moiz.sajid@tum.de

Technische Universität München



Figure 1: Reconstruction pipeline used in this project: RGB-D Frame Capture, Correspondence Finding, Camera Calibration, Voxelgrid TSDF, Marching Cubes

Abstract

Our goal in this project is to get a real time mesh reconstruction of dynamic scenes using a multi view camera capture setup. We use three Intel RealSense D415 depth cameras for RGB-D data capturing which are calibrated using known correspondences from markers. The data is fused into a voxelgrid representing the implicit surface and following a marching cubes algorithm is performed for the final surface extraction. Both qualitative and quantitative results are presented.

1. Introduction

Volumetric Capture is an extensively researched topic where the goal is to get an accurate 3D reconstruction of dynamic scenes in real time. The first work in the area was done by Cureless and Levoy [1] in which they integrated data from one range image into a cumulative weighted signed distance function. KinectFusion [8] was another milestone in this area which proposed a real time mapping system of indoor scenes using a single depth camera. DynamicFusion [7] handles non-rigid scenes and reconstruction over time. Our work mostly focuses on reconstructing dynamic scenes on a per frame basis.

One application area of our project is Holoportation [13] where 3D reconstructed models are used for VR interactions between two persons over huge distances.

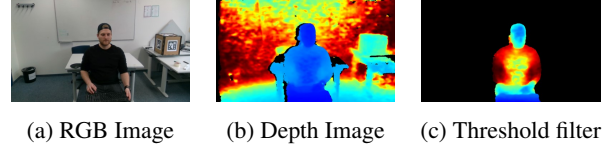


Figure 2: The color and depth images captured by the cameras

2. Reconstruction Pipeline

To perform the real time 3D reconstruction we implemented the pipeline which is exemplary displayed in Figure 1 and described in the following section.

All tests were performed on a Laptop with an Intel® Core™ i7-6700HQ CPU @ 2.60GHz [3], 40GB of DDR4 RAM and a Nvidia GeForce GTX 970M [9].

2.1. RGB-D Frame Capture

We use three Intel® RealSense™ Depth Camera D415 [4] for our capture setup which work on the concept of active stereo depth. Two cameras are placed on the sides of the camera and the depth is calculated from a triangulation using the displacement. An infrared pattern is projected into the scene to enhance the details.

We process the depth images using a threshold filter which discards pixels that are above or below a threshold set during runtime. We also tried different hole-filling, spatial and edge enhancing filters that did not improve the results and are not used in the final reconstruction.

Figure 2 displays the raw RGB-D images and the filtered depth image.

We tried to extend the three camera setup with a fourth one but were not able to integrate it due to bandwidth limitations. Furthermore, we had to limit the color and depth resolutions as well as framerates to enable three cameras and to allow a processing of the data in real time. The resolution we used for the color and depth stream is 848x480 px at 30 frames per second. [6] gives more detail about the limitations of the cameras in a multi camera setup.

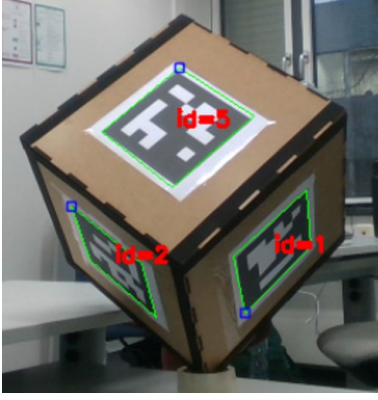


Figure 3: Marker cube with the detected markers highlighted in green and their unique identifiers (red).

The RGB-D images from the three cameras are time synchronized [6] what improves the results of the following camera calibration and the final mesh reconstruction.

Intel[©] provides an excellent SDK [5], good support and updates for its API which made it easy to use the cameras.

2.2. Correspondence Finding

We use ArUco markers [10] to find correspondences between the three camera streams. These markers have a unique identifier and can easily be detected in every color image using the OpenCV [12] library. The markers are mounted on a wooden cube box as shown in Figure 3.

By placing the cameras such that each one is looking on one of the cubes corners we can assure that in every color image three markers are visible. This also ensures that between every pair of cameras we have an overlap of two markers for which the eight corner positions are detected sub pixel perfect. This gives us a total of $8 * 3 = 24$ constraints between every pair of cameras which are used in the next step to estimate the relative transformation between the markers.

It is also important to mention here that we tried ChArUco markers [11] which are a mixture of ArUco markers [10] and a chessboard pattern which allow simultaneous detection and pose estimation. However, the ChArUco markers [11] did not give us good pose results, so we stick to ArUco markers [10].

2.3. Camera Calibration

After getting the marker locations, we backprojected these correspondences into the 3D pointcloud using the depth information. The camera poses of the cameras were then estimated using OpenCV. Using these camera poses, we calculated relative transformations between the cameras.

Out of three camera, we selected the first camera's coordinate frame as the world coordinate frame and hence the poses from the other two cameras were aligned with respect to the first camera. The alignment we got from the camera calibration was not good which meant that it can be improved further.

2.4. Optimization

As the pose parameters that we got from the camera calibration were not good enough, we used two different optimizations approaches namely Procrustes and Point-to-Point correspondence error for optimizing the 3D pose parameters of the cameras even further.

In the Procrustes algorithm, we compute the vector between the center of gravity for getting the translation components and the Singular Value Decomposition of the known correspondences for getting the rotation components as shown in Equation (1) and (2). The alignment that we get from Procrustes is not robust enough and hence has a high Mean Squared Error (MSE).

$$USV^T = SVD(X^T X) \quad (1)$$

$$R = UV^T \quad (2)$$

In order to further improve the results that we get from Procrustes, we used the Point-to-Point correspondence error. For the Point-to-Point correspondence error, we optimize for the following energy term:

$$\sum_i \sum_j \sum_k \|(X_{ik} - T_j R_j * X_{jk})\|_2^2 \quad (3)$$

Further results have been summarized in Table 1. One of the difficulties that we faced in camera calibration was visualizing the aligned points for which we had to write our own rendering pipeline in OpenGL [14]. Another difficulty that we faced was with Ceres because we had to get ourselves acquainted with general working of the non-linear optimization framework.

2.5. Voxelgrid TSDF

Once we have these aligned pointclouds, we fuse them into the voxelgrid. We project the voxelgrid into the depth frame of the camera and we calculate the difference by subtracting the voxel depth from the actual depth value using Equation (4). For the truncated signed-distance function (tsdf) values we did the weighted averaging using the Equation (5). The tsdf values were truncated between -1 and 1 with points having a negative value inside the surface and positive value outside the surface.

$$tsdf = z_{voxel} - z_{depth} \quad (4)$$

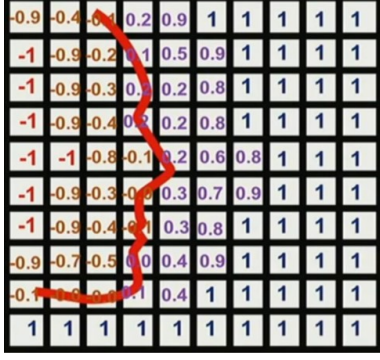


Figure 4: TSDF Representation

$$tsdf_{i+1} = \frac{tsdf_i * weight}{weight + 1} \quad (5)$$

Given that we were using a large number of gridpoints, computing tsdf values on the CPU was not feasible. So we had to move our tsdf voxelgrid implementation onto the GPU inorder to achieve real time results. Since we were already using OpenGL for the rendering pipeline, we decided to use OpenGL Compute Shaders [2] for parallelizing the tsdf voxelgrid implementation. We also had to find a tradeoff between voxel resolution and frame rate. With a lower voxel resolution, the frame rate dropped because more calculations had to be done. Furthermore, finding a good truncation distance was also very crucial for lowering the artefacts. The Table 2 summarizes the time comparisons between different voxel resolutions.

2.6. Surface Extraction

For the iso-surface extraction, we used the Marching Cubes algorithm which converts the implicit surface representation to a polygonal mesh. We then iterated over the voxelgrid cells to determine the zero crossings and looked up the triangulation in the Marching Cubes table. This gives us the triangulated mesh as a final output. With a lower voxel resolution and more grid points, we were able to get more finer reconstruction. Again we had to utilize the OpenGL Compute Shader in order to achieve real time results because the computations on the CPU were really slow.

Intially, we had voxelgrid points that were not initialized because they were outside the camera view. As a result, we had a huge number of artefacts in the final mesh reconstruction which took a lot of time to figure out. We implemented a two pass OpenGL Compute Shader. In the first pass, we counted the number of triangles that will generated and only allocated space for them. In the second pass, we generate the triangles. We do this because the upper bound for the number of generated triangle is five times the number of voxelgrid points. For example if we have 200x200x200 grid



Figure 5: Result with using only one camera

points with a 5 millimeter voxel resolution, we roughly had 40 million number of possible triangles. We only generated a fraction of these triangles after the the triangle counting OpenGL Compute Shader pass. For a voxel resolution of 5mm resolution, the Marching Cubes algorithm took 15 milliseconds which was real time capable. For 3 millimeter resolution, the results were not real time capable however, we were to get fine mesh reconstructions. The Table 2 summarizes the time comparisons between different voxel resolution. The Table 3 summarizes the time comparisons for running Marching Cubes between different voxel resolutions.

3. Results

The results that we get using one camea are really good as can be seen in Figure 5. Figure 6 displays the triangulation results using one camera. However, we get artefacts when we use all three camera streams. The which artefacts which are mostly visible around the edges can be seen in Figure 7. This suggests that the camera pose parameters can be improved further.

Algorithm	Iterations	Duration [ms]	MSE
Procrustes (A)	1	8 - 20	<0.7 - 1.73
Point-to-Point (A)	1 - 20	900 - 1000	<0.1
Procrustes (C)	1	20 - 40	0.25 - 1.29
Point-to-Point (C)	1 - 20	18000 - 22000	<0.1

Table 1: Comparisons between different optimization algorithms in terms of iterations, duration and MSE (Mean Squared Error). A=ArUco and C=ChArUco



Figure 6: Triangulation result with using only one camera



Figure 7: Result with using three cameras

Algorithm	Resolution [mm]	Gridpoints	Duration [ms]
All frames	20	125,000	<1
All frames	10	1,000,000	<1
All frames	5	8,000,000	5
All frames	4	15,625,000	20
All frames	3	37,000,000	50

Table 2: Time comparisons for calculating voxelgrid of different voxel resolutions as well as the number of gridpoints used. The voxelgrid measured 1 meter x 1 meter x 1 meter.

4. Future Work and Conclusion

Since we optimized for pose parameters for a limited number of markers, one of the further improvements that we can do in camera calibration is to use more correspondences which can found for example by using Nearest Neighbor Search and then use the Global Alignment techniques like

Resolution [mm]	Duration [ms]	Gridpoints
20	<1	7,000 - 10,000
10	<1	40,000 - 45,000
5	15	200,000 - 250,000
4	35	380,000 - 420,000
3	80	600,000 - 800,000

Table 3: Time comparisons for running the Marching Cubes on different voxel resolutions. The number of triangles generated are also displayed.

Iterative Closest Points (ICP).

5. Group Member Contributions

References

- [1] B. Curless and M. Levoy. A volumetric method for building complex models from range images. *ACM SIGGRAPH*, 1996.
- [2] A. Gerdelan. It's more fun to compute: An introduction to compute shaders. <http://antongerdelan.net/opengl/compute.html>, 2016. Accessed: 10.02.2020.
- [3] Intel®. Intel® core™ i7-6700HQ processor. <https://ark.intel.com/content/www/de/de/ark/products/88967/intel-core-i7-6700hq-processor-6m-cache-up-to-3-50-g.html>. Accessed: 19.02.2020.
- [4] Intel®. Intel® realsense™ depth camera d415. <https://www.intelrealsense.com/depth-camera-d415/>. Accessed: 19.02.2020.
- [5] Intel®. Intel® realsense™ sdk. <https://www.intelrealsense.com/developers/>. Accessed: 19.02.2020.
- [6] Intel®. Using the intel® realsense™ depth camera d4xx in multi-camera configurations. https://www.intel.com/content/dam/support/us/en/documents/emerging-technologies/intel-realsense-technology/RealSense_Multiple_Camera_WhitePaper.pdf. Accessed: 19.02.2020.
- [7] R. A. Newcombe, D. Fox, and S. M. Seitz. Dynamicfusion: Reconstruction and tracking of non-rigid scenes in real-time. *IEEE CVPR*, 2015.
- [8] R. A. Newcombe, S. Izadi, O. Hilliges, D. Molyneaux, D. Kim, A. J. Davison, P. Kohli, J. Shotton, S. Hodges, and A. Fitzgibbon. Kinectfusion: Real-time dense surface mapping and tracking. *IEEE ISMAR*, 2011.
- [9] Nvidia. Geforce gtx 970m. <https://www.geforce.com/hardware/notebook-gpus/geforce-gtx-970m>. Accessed: 19.02.2020.
- [10] OpenCV. Detection of aruco markers. https://docs.opencv.org/trunk/d5/dae/tutorial_aruco_detection.html. Accessed: 19.02.2020.

- [11] OpenCV. Detection of charuco corners. https://docs.opencv.org/3.4/df/d4a/tutorial_charuco_detection.html. Accessed: 19.02.2020.
- [12] OpenCV. Opencv. <https://opencv.org/>. Accessed: 19.02.2020.
- [13] S. Orts-Escolano, C. Rhemann, S. Fanello, W.Chang, A. Kowdle, Y. Degtyarev, David Kim, P. Davidson, S. Khamis, M. Dou, V. Tankovich, C. Loop, Q. Cai, P. Chou, S. Menickken, J. Valentin, V. Pradeep, S. Wang, S. Bing Kang, P. Kohli, Y. Lutchyn, C. Keskin, and S. Izadi. Holoportation: Virtual 3d teleportation in real-time. *ACM User Interface Software and Technology Symposium (UIST)*, 2016.
- [14] J. Vries. Learnopengl. <https://learnopengl.com/>, 2015. Accessed: 10.02.2020.